Eur. Phys. J. B (2018) 91: 286
https://doi.org/10.1140/epjb/e2018-90179-4

THE EUROPEAN PHYSICAL JOURNAL B

Regular Article

Termini effects on the optical properties of graphene nanoribbons*

Claudia Cardoso[a], Andrea Ferretti, and Deborah Prezzi[b]

CNR-Nanoscience Institute, S3 Center, via G. Campi 213/a, 41125 Modena, Italy

Received 16 March 2018 / Received in final form 6 September 2018
Published online 19 November 2018

Abstract. We investigate from first principles the optical response of finite-length armchair-edged graphene nanoribbons (AGNRs) within the framework of many-body perturbation theory. As a result of the explicit inclusion of zigzag extremities, we identify low-energy and low-intensity excitations that are expected to be almost independent of the GNR length. These excitations coexist with bulk-like excitations, which have the same origin as the ones characterizing infinite AGNRs. Our results are used to rationalize termini effects on the optical response of GNRs and to shed light on recent photoluminescence data.

1 Introduction

Owing to the predicted width- and chirality-dependent tunable bandgaps [1–3], as well as to their peculiar optical response [2,4–6], graphene nanoribbons (GNRs) have attracted increasing attention in the last decade as a viable route for the implementation of graphene-based electronic and opto-electronic devices. More recently, the successful production of ultranarrow and structurally well-defined GNRs by means of bottom-up techniques [7,8] has further boosted this research line. Not only the most studied armchair (A-) [9] and zigzag (Z-) [10] GNRs have been produced, but also GNRs with more complex edge morphology [9,11] and functionalization [12–14], where the realization of a fine-tuning of the GNR properties is demonstrated by on-purpose design of their molecular building blocks.

For these atomically precise nanostructures, sizeable electronic bandgaps have been reported [13,15–20], together with important achievements towards the realization of seamless heterojunctions [21,22] and field-effect transistor (FET) configurations [23,24]. In addition, their optical response has been demonstrated to be dominated by pronounced excitonic effects [25,26]. Biexciton formation has been shown to play a key role in the high-excitation regime [27], and huge trion binding energies have been reported from theoretical modelling [28]. The characterization of GNR absorbance reflects the tunability of the bandgap, with the optical onset ranging from near IR to the visible, while varying the specific GNR atomic structure [13,25,26,29,30]. Their luminescence properties, of key importance for applications in light-emitting devices, are instead less deeply understood, with different results depending on both GNR structure and external conditions [31–35]. In particular, recent STM-induced light emission experiments [35] on individual 7-AGNRs reveal sharp, below-bandgap luminescence, pointing to the key role of the states localized at the GNR-zigzag termini. On the contrary, ensemble measurements for the same systems on quartz show weak and featureless emission spectra [34], which are attributed to the presence of dark states.

Indeed, the absorption properties of GNRs have been modelled so far by using truly infinite systems, and successfully compared with experiments [13,25–27]. However, finite-length effects may become relevant when considering the emission process, as demonstrated in reference [35]. Here, we investigate the optical properties of the pristine 7-AGNR in gas-phase by focusing on the effects arising for the presence of zigzag-termined ends. We model the system by considering a 2-nm-long 7-AGNR (see Fig. 1, bottom), and its optical spectrum is simulated by means of ab initio calculations within the GW plus Bethe–Salpeter equation (BSE) framework. Our results indicate that the linear optical response is characterized by low-energy excitations involving localized states at the GNR termini, as well as by bulk excitations, which arise from transitions between states delocalized along the GNR. Recent experimental observations are finally discussed in the light of our findings.

* Contribution to the Topical Issue "Special issue in honor of Hardy Gross", edited by C.A. Ullrich, F.M.S. Nogueira, A. Rubio, and M.A.L. Marques.

[a] *Present address:* International Iberian Nanotechnology Laboratory, Avenida Mestre José Veiga s/n 4715-330 Braga, Portugal.

[b] e-mail: deborah.prezzi@nano.cnr.it

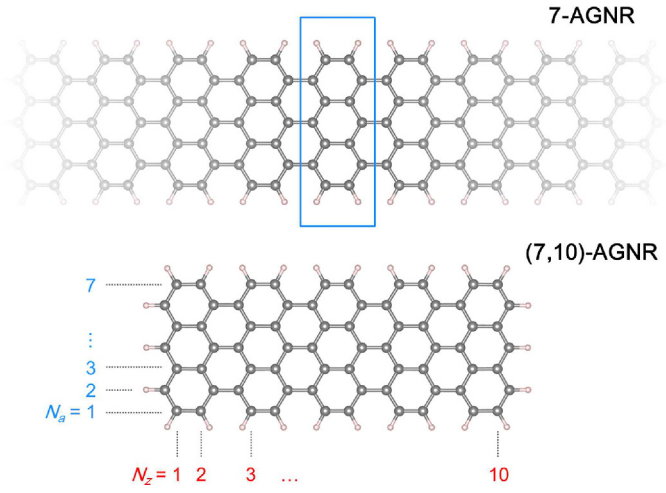

Fig. 1. Ball-and-stick model of an infinite 7-AGNR (top, periodic unit cell is highlighted by the blue box) and a finite-length (7,10)-AGNR (bottom). Width (N_a) and length (N_z) parameters are indicated in blue and red, respectively.

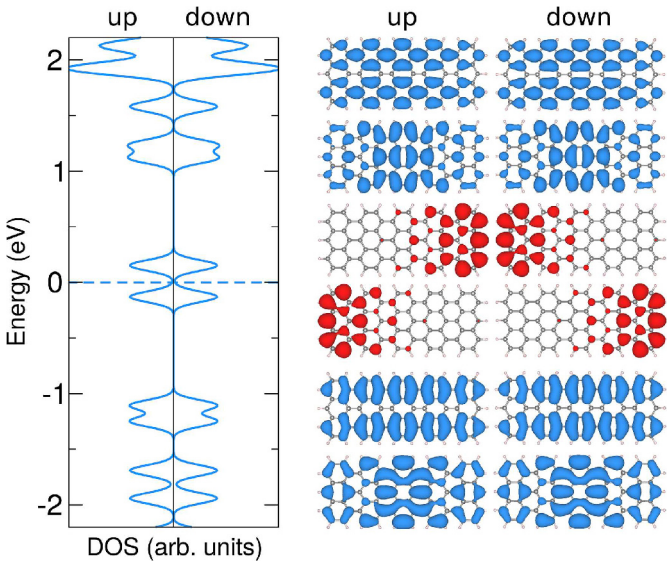

Fig. 2. Density of states (DOS) of (7,10)-AGNR according to the DFT–LSDA description (left), together with a few representative molecular orbitals around the Fermi level (right).

2 Computational methods

Simulations of the ground-state structural and electronic properties of finite-length 7-AGNR were performed using a first-principles supercell implementation of density functional theory (DFT) based on plane waves and pseudopotentials, as available in the QUANTUM ESPRESSO package [36,37]. The local spin-density approximation (LSDA, Perdew–Zunger parametrization [38]) was adopted for the exchange correlation potential, together with norm conserving pseudopotentials, with a 80-Ry energy cutoff on the wavefunctions. The supercell size was set to be at least twice the length and width of the studied ribbons, while the distance between the ribbon planes was set to at least 12 Å, in order to prevent interaction between periodic replicas (note that the supercell size was chosen already at the DFT level to comply with the constraints for box-shaped truncation of the Coulomb potential – see below). Atomic positions were fully relaxed until forces were smaller than 0.026 eV/Å.

The optical absorption properties were subsequently computed within the framework of many-body perturbation theory [39], according to the GW-BSE approach. Quasiparticle corrections to the Kohn–Sham eigenvalues were calculated within the G_0W_0 approximation for the self-energy operator, where the dynamic dielectric function was obtained within the plasmon-pole approximation [40]. The Coulomb potential was hereafter truncated by using a box-shaped cutoff to remove the long-range interaction between periodic images and simulate isolated systems. The sum-over-states in the calculation of polarizability operator (self-energy) was truncated at 1200 bands, respectively, with the usage of Bruneval–Gonze terminator approach [41]; a cutoff of 3 Ry was employed to represent the response function.

The gas-phase optical absorption spectra were then computed as the imaginary part of the macroscopic dielectric function starting from the solution of BS equation in order to take into account electron–hole (e–h) interaction. The static screening in the direct term was calculated within the random-phase approximation, by including 1200 bands in the sum-over-states and 3 Ry for the reciprocal space representation of the polarizability operator. The optical absorption spectra were calculated including 30 valence bands and 20 conduction bands, together with the application of Tamm–Dancoff approximation. Note that full spin-polarization is considered for the description of both ground- and excited-state properties in order to capture the antiferromagnetic ordering found for these systems [42,43]. Both GW and BSE calculations were performed with the YAMBO code [44].

3 Results

Figure 1 shows the comparison between infinite (top) and finite-length AGNR (bottom) geometries. Following the standard nomenclature [43], finite-length AGNRs are labelled according to both their width and length parameters, i.e. (N_a, N_z)-AGNRs, where N_a is the number of dimeric lines across their width, as for infinite GNRs, and N_z is the number of zigzag lines along their length. Here we focus on a (7,10)-AGNR with fully monohydrogenated edges, which is less than 1-nm wide and about 2-nm long. Similar short AGNRs have been recently synthesized on Au(111) by bottom-up approaches [43], and STS investigations of their electronic properties indicate the cohexistence of bulk-like states, delocalized along the GNR and Tamm-like states localized at the zigzag ends, as also predicted by theoretical modelling [42].

In Figure 2 (left-hand side) we report the DFT–LSDA density of states (DOS) for the (7,10)-AGNR. Indeed, the two zigzag termini are antiferromagnetically coupled, and each of them gives rise to a pair of spin–split, localized

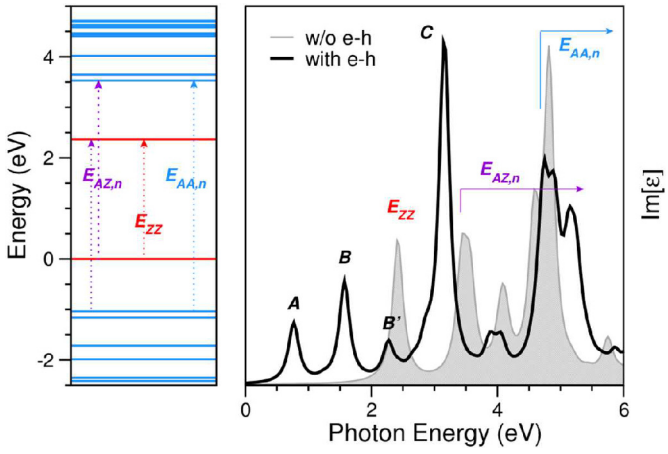

Fig. 3. Left: GW-corrected energy level scheme of (7,10)-AGNR. Tamm states are displayed in red, while bulk-like states are in blue. Right: Optical absorption spectrum of (7,10)-AGNR. The independent particle spectrum is in grey (shaded area), whereas the spectrum including e–h interaction at the BSE level is reported in black.

states (red molecular orbitals on the right-hand side of Fig. 2) that lie in the gap formed by the bulk delocalized orbitals (in blue), in agreement with experimental observations and previous theoretical findings [42,43]. Similar results have been also reported for GNRs with extended zigzag edges, which present an antiferromagnetic ground state with the last valence and the first conduction (doubly degenerate) bands localized at the zigzag edges [45,46].

For the case of (7,10)-AGNR, the DFT-LSDA energy gap between occupied and empty doubly degenerate Tamm states, i.e. Δ_{ZZ}, is about 0.28 eV, while the energy separation of bulk states, i.e. Δ_{AA}, is larger than 2 eV. The inclusion of quasiparticle corrections, as resulting from G_0W_0 calculations (see Sect. 2), brings Δ_{ZZ} to a value of 2.37 eV, i.e. more than eight times larger than the DFT–LSDA one (see Fig. 3). These corrections are significantly larger than for extended Z-GNRs [4], where GW gaps exceed by about three times the DFT–LSDA ones (e.g. from 0.3 to 1.0 eV for the 10-Z-GNR). This is due to the additional confinement of the Tamm states along the zigzag direction, as also suggested in reference [43]. Our results are in overall good agreement with previous GW calculations for different (7,N_z)-AGNRs [43], and we have checked that quantitative differences have to be completely attributed to the different starting point for G_0W_0 calculations, i.e. LDA vs. PBE.

The G_0W_0-corrected energy levels (Fig. 3, left-hand side) and the DFT–LSDA wave functions are the ingredients for the calculation of optical absorption of the system, which is depicted in Figure 3 (right-hand side). The independent-particle spectrum (grey area) is characterized by three main types of features: the E_{ZZ} peak at 2.37 eV, corresponding to the transition between Tamm states (in red); the $E_{AZ,n}$ series of transitions from occupied bulk (Tamm) states to Tamm (bulk) empty states, starting from about 3.4 eV; the $E_{AA,n}$ series of transitions between bulk states, starting from about 4.7 eV. The inclusion of excitonic effects (black curve) alters significantly both energies and shape of the spectrum, as also found for infinite 7-AGNRs [25]. The spectrum is indeed significantly redshifted, with an exciton binding energy for the lowest-energy A peak of 1.60 eV. More in detail, the two lowest energy excitations (at 0.64 and 0.77 eV) are mainly given by a dark and an optically active (A peak) combination of the E_{ZZ} transition; the high-energy features giving rise to the B/B' and C peaks derive instead from the linear combination of $E_{AZ,n}$ and $E_{AA,n}$ transitions, respectively.

4 Discussion and conclusions

Let us now compare the above results for finite AGNRs with the optical response of extended Z- and AGNRs. It is worth noting that excitations similar to the ones contributing to the A and B peaks (i.e. arising from E_{ZZ} and $E_{AZ,n}$ transitions, respectively) constitute the main optical features of extended Z-GNRs [5], even though with a much larger exciton binding energy here (1.7 vs. 0.7 eV) in view of the additional confinement along the zigzag direction. Moreover, we find here the C peak, arising from the linear combination of transitions between bulk states, is the finite size analogous to the main excitations characterizing infinite 7-AGNRs. Again quantum confinement along the armchair (length) direction plays a key role. In fact, the energy position of the C peak (about 3 eV) is much higher than that of its analogous in infinite 7-AGNRs (about 2 eV) [25]. Previous calculations [35,47] not including the spin polarization have shown that the energy position of bulk-like excitations tends to that of infinite AGNRs only for lengths well-above 3 nm, i.e. exceeding significantly the exciton Bohr radius of the lowest bulk excitations. For such lengths, we also expect the intensity of the A and B peaks to become less prominent or negligible in view of the reduced overlap between the single-particle states; their energy position should instead vary very little, in view of the localized nature of the single-particle transitions participating in their composition. Previous calculations and STS measurements indicate that the quasiparticle gap between Tamm states is indeed independent of the GNR length already for $N_z = 10$ [43].

The above considerations can also give us some insight on the available experimental findings. Concerning optical absorption, the agreement between experimental observation and theoretical modelling for infinite systems is very good for 7-AGNRs [25], and there are no reports of low energy features below 2 eV as those reported here (A and B peaks). This is reasonable in view of the typical length of GNRs (on the order of 20 nm or longer [15]): in these cases the intensity of low-energy peaks involving Tamm states is expected to be strongly suppressed by the small overlap, as discussed above. While calculations in this regime are prohibitive, it would be interesting to have optical measurements on short 7-AGNRs as those reported in reference [43] in order to possibly probe these low-energy excitations involving Tamm states in a range

where the overlap between single-particle states is still substantial.

At variance with absorption, light emission for the same systems has not been fully understood yet. Recently, below-bandgap, bright emission at about 1.2 eV has been observed for individual 7-AGNRs lifted between a STM tip and a Au substrate [35], and the key role of Tamm states localized at the zigzag termini has been pointed out by comparison with ab initio theoretical modelling. In this case the lowest energy peak (A) arising from transitions between Tamm states is not expected to be seen, since the contact with gold STM tip is found to wash out the magnetic character of the excitations, thus closing the Δ_{ZZ} gap; $E_{AZ,n}$ transitions remain instead active, and the emission features – observed experimentally, thanks to the tip enhancement – have been indeed attributed to transitions between Tamm and bulk states (i.e. the equivalent of B peak here).

At variance with the above cited measurements on individual GNRs [35], ensemble measurements on 7-AGNRs transferred on quartz display weak and featureless emission [34], and the low-quantum yield is attributed to the presence of a dark state below the first bright one for the $N_a = 3p + 1$ family of AGNRs, as predicted for $N_a = 10$ [2,4]. However, for $N_a = 7$ this optically inactive state results to be 50 meV above the first bright [6,25]. Hence, according to theoretical predictions for infinite systems, the 7-AGNRs should display bright emission at about 2 eV. The present results, which include explicitly the zigzag termini, show instead the appearance of several below-bandgap excitations, which are expected to have negligible optical activity for long GNRs, as discussed above, and could be at the origin of the weak emission spectra reported in reference [34]. Our results can thus help reconciling the different experimental observations published so far on 7-AGNRs, fully elucidating their origin.

In conclusion, we have investigated the linear optical response of short 7-AGNRs by means of ab initio many-body perturbation-theory-based techniques, including both electron–electron and electron–hole interactions. We find three types of excitations, that is, excitons localized at the zigzag termini, excitons mixing transitions between bulk and Tamm states, and fully bulk-like excitations, similar to those found for extended GNRs. The properties of these excitations are analyzed in comparison to those of the excitations characterizing the extended Z- and AGNRs and used to gain further insights into the most recent experimental observations, clarifying the key role of Tamm states localized at the zigzag termini in determining the optical properties of AGNRs.

This work was financially supported by the European Union H2020-EINFRA-2015-1 program (Grant No. 676598, project MaX – MAterials at the eXascale). Computational resources were provided by the ISCRA program (Grant No. HP10BO7B2W) and by PRACE via project SHINE (Grant No. Pra11_2921) on the Marconi machine at CINECA. The authors thank D. Sangalli for fruitful discussion.

Author contribution statement

D.P. and A.F. conceived the theoretical study. C.C. carried out the simulations. D.P. wrote the manuscript with contributions from all authors. All authors discussed the results and commented on the manuscript at all stages, reading and approving the final manuscript.

References

1. L. Yang, C.H. Park, Y.W. Son, M.L. Cohen, S.G. Louie, Phys. Rev. Lett. **99**, 186801 (2007)
2. D. Prezzi, D. Varsano, A. Ruini, A. Marini, E. Molinari, Phys. Rev. B **77**, 041404 (2008)
3. S. Osella, A. Narita, M.G. Schwab, Y. Hernandez, X. Feng, K. Müllen, D. Beljonne, ACS Nano **6**, 5539 (2012)
4. L. Yang, M.L. Cohen, S.G. Louie, Nano Lett. **7**, 3112 (2007)
5. L. Yang, M.L. Cohen, S.G. Louie, Phys. Rev. Lett. **101**, 186401 (2008)
6. D. Prezzi, D. Varsano, A. Ruini, E. Molinari, Phys. Rev. B **84**, 041401 (2011)
7. A. Narita, X. Feng, K. Müllen, Chem. Rec. **15**, 295 (2015)
8. A. Narita, X.Y. Wang, X. Feng, K. Müllen, Chem. Soc. Rev. **44**, 6616 (2015)
9. J. Cai, P. Ruffieux, R. Jaafar, M. Bieri, T. Braun, S. Blankenburg, M. Muoth, A.P. Seitsonen, M. Saleh, X. Feng, et al., Nature **466**, 470 (2010)
10. P. Ruffieux, S. Wang, B. Yang, C. Sánchez-Sánchez, J. Liu, T. Dienel, L. Talirz, P. Shinde, C.A. Pignedoli, D. Passerone, et al., Nature **531**, 489 (2016)
11. A. Narita, X. Feng, Y. Hernandez, S.A. Jensen, M. Bonn, H. Yang, I.A. Verzhbitskiy, C. Casiraghi, M.R. Hansen, A.H.R. Koch et al., Nat. Chem. **6**, 126 (2014)
12. A. Keerthi, B. Radha, D. Rizzo, H. Lu, V. Diez Cabanes, I.C.Y. Hou, D. Beljonne, J. Cornil, C. Casiraghi, M. Baumgarten, et al., J. Am. Chem. Soc. **139**, 16454 (2017)
13. Y. Hu, M. De Corato, A. Ruini, S. Zhao, F. Meggendorfer, L.A. Straasø, L. Rondin, P. Simon, J. Li, J. Finley, et al., J. Am. Chem. Soc. **140**, 7803 (2018)
14. R.A. Durr, D. Haberer, Y.L. Lee, R. Blackwell, A.M. Kalayjian, T. Marangoni, J. Ihm, S.G. Louie, F.R. Fischer, J. Am. Chem. Soc. **140**, 807 (2018)
15. P. Ruffieux, J. Cai, N.C. Plumb, L. Patthey, D. Prezzi, A. Ferretti, E. Molinari, X. Feng, K. Müllen, C.A. Pignedoli, et al., ACS Nano **6**, 6930 (2012)
16. S. Linden, D. Zhong, A. Timmer, N. Aghdassi, J.H. Franke, H. Zhang, X. Feng, K. Müllen, H. Fuchs, L. Chi, et al., Phys. Rev. Lett. **108**, 216801 (2012)
17. Y.C. Chen, D.G. de Oteyza, Z. Pedramrazi, C. Chen, F.R. Fischer, M.F. Crommie, ACS Nano **7**, 6123 (2013)
18. A. Kimouche, M.M. Ervasti, R. Drost, S. Halonen, A. Harju, P.M. Joensuu, J. Sainio, P. Liljeroth, Nat. Commun. **6**, 10177 (2015)
19. H. Zhang, H. Lin, K. Sun, L. Chen, Y. Zagranyarski, N. Aghdassi, S. Duhm, Q. Li, D. Zhong, Y. Li, et al., J. Am. Chem. Soc. **137**, 4022 (2015)
20. L. Talirz, H. Söde, T. Dumslaff, S. Wang, J.R. Sanchez-Valencia, J. Liu, P. Shinde, C.A. Pignedoli, L. Liang, V. Meunier, et al., ACS Nano **11**, 1380 (2017)

21. J. Cai, C.A. Pignedoli, L. Talirz, P. Ruffieux, H. Söde, L. Liang, V. Meunier, R. Berger, R. L, X. Feng, et al., Nat. Nanotechnol. **9**, 896 (2014)
22. Y.C. Chen, T. Cao, C. Chen, Z. Pedramrazi, D. Haberer, D.G. de Oteyza, F.R. Fischer, S.G. Louie, M.F. Crommie, Nat. Nanotechnol. **10**, 156 (2015)
23. P.B. Bennett, Z. Pedramrazi, A. Madani, Y.C. Chen, D.G. de Oteyza, C. Chen, F.R. Fischer, M.F. Crommie, J. Bokor, Appl. Phys. Lett. **103**, 253114 (2013)
24. J.P. Llinas, A. Fairbrother, G. Borin Barin, W. Shi, K. Lee, S. Wu, B. Yong Choi, R. Braganza, J. Lear, N. Kau, et al., Nat. Commun. **8**, 633 (2017)
25. R. Denk, M. Hohage, P. Zeppenfeld, J. Cai, C.A. Pignedoli, H. Söde, R. Fasel, X. Feng, K. Müllen, S. Wang et al., Nat. Commun. **5**, 4253 (2014)
26. R. Denk, A. Lodi-Rizzini, S. Wang, M. Hohage, P. Zeppenfeld, J. Cai, R. Fasel, P. Ruffieux, R. Berger, Z. Chen, et al., Nanoscale **9**, 18326 (2017)
27. G. Soavi, S. Dal Conte, C. Manzoni, D. Viola, A. Narita, Y. Hu, X. Feng, U. Hohenester, E. Molinari, D. Prezzi, et al., Nat. Commun. **7**, 11010 (2016)
28. T. Deilmann, M. Rohlfing, Nano Lett. **17**, 6833 (2017)
29. H.E. Lim, Y. Miyata, M. Fujihara, S. Okada, Z. Liu, Arifin, K. Sato, H. Omachi, R. Kitaura, S. Irle, et al., ACS Nano **9**, 5034 (2015)
30. A. Narita, I.A. Verzhbitskiy, W. Frederickx, K.S. Mali, S.A. Jensen, M.R. Hansen, M. Bonn, S. De Feyter, C. Casiraghi, X. Feng, et al., ACS Nano **8**, 11622 (2014)
31. A.I. Chernov, P.V. Fedotov, A.V. Talyzin, I. Suarez Lopez, I.V. Anoshkin, A.G. Nasibulin, E.I. Kauppinen, E.D. Obraztsova, ACS Nano **7**, 6346 (2013)
32. S. Zhao, L. Rondin, G. Delport, C. Voisin, U. Beser, Y. Hu, X. Feng, K. Müllen, A. Narita, S. Campidelli, et al., Carbon **119**, 235 (2017)
33. S. Zhao, G. Borin Barin, L. Rondin, C. Raynaud, A. Fairbrother, T. Dumslaff, S. Campidelli, K. Müllen, A. Narita, C. Voisin, et al., Phys. Stat. Sol. B **254**, 1700223 (2017)
34. B.V. Senkovskiy, M. Pfeiffer, S.K. Alavi, A. Bliesener, J. Zhu, S. Michel, A.V. Fedorov, R. German, D. Hertel, D. Haberer, et al., Nano Lett. **17**, 4029 (2017)
35. M.C. Chong, N. Afshar-Imani, F. Scheurer, C. Cardoso, A. Ferretti, D. Prezzi, G. Schull, Nano Lett. **18**, 175 (2018)
36. P. Giannozzi, S. Baroni, N. Bonini, M. Calandra, R. Car, C. Cavazzoni, D. Ceresoli, G.L. Chiarotti, M. Cococcioni, I. Dabo, et al., J. Phys. Condens. Matter **21**, 395502 (2009)
37. P. Giannozzi, O. Andreussi, T. Brumme, O. Bunau, M.B. Nardelli, M. Calandra, R. Car, C. Cavazzoni, D. Ceresoli, M. Cococcioni, et al., J. Phys. Condens. Matter **29**, 465901 (2017)
38. J.P. Perdew, A. Zunger, Phys. Rev. B **23**, 5048 (1981)
39. G. Onida, L. Reining, A. Rubio, Rev. Mod. Phys. **74**, 601 (2002)
40. R.W. Godby, R.J. Needs, Phys. Rev. Lett. **62**, 1169 (1989)
41. F. Bruneval, X. Gonze, Phys. Rev. B **78**, 085125 (2008)
42. M. Golor, C. Koop, T.C. Lang, S. Wessel, M.J. Schmidt, Phys. Rev. Lett. **111**, 085504 (2013)
43. S. Wang, L. Talirz, C.A. Pignedoli, X. Feng, K. Müllen, R. Fasel, P. Ruffieux, Nat. Commun. **7**, 11507 (2016)
44. A. Marini, C. Hogan, M. Grüning, D. Varsano, Comput. Phys. Commun. **180**, 1392 (2009)
45. K. Nakada, M. Fujita, G. Dresselhaus, M.S. Dresselhaus, Phys. Rev. B **54**, 17954 (1996)
46. Y.W. Son, M.L. Cohen, S.G. Louie, Phys. Rev. Lett. **97**, 216803 (2006)
47. C. Cocchi, D. Prezzi, A. Ruini, E. Benassi, M.J. Caldas, S. Corni, E. Molinari, J. Phys. Chem. Lett. **3**, 924 (2012)